Invited Paper

Physical Phenomena and Length Scales Governing the Behaviour of Wildfires: A Case for Physical Modelling

Dominique Morvan*, Laboratoire de Mécanique, Modélisation & Procédés Propres (M2P2), UMR CNRS-Universités de Marseille, Université de la Méditerranée UNIMECA, 60 Rue Joliot Curie Technopôle de Château Gombert, 13453 Marseille Cedex 13, France

Abstract. This paper is an overview of the physical mechanisms and length scales governing the propagation of wildfires. One of the objectives is to identify the physical and mathematical constraints in the modelling of wildfires when using a "fully" physical approach. The literature highlights two regimes in the propagation of surface fires, i.e. wind-driven fires and plume-dominated fires, which are governed by radiation and convective heat transfer, respectively. This division leads to the identification of two governing length scales: the extinction length characterising the absorption of radiation by vegetation, and the integral turbulent length scale characterising the interaction between wind and canopy. Some numerical results published during the last decade using a fully physical approach are presented and discussed with a focus on the models FIRESTAR, FIRELES, FIRETEC and WFDS. Numerical simulations were compared with experimental data obtained at various scales, from laboratory to field fires in grassland and in Mediterranean shrubland. Some perspectives are presented concerning the potential coupling between physical fire models with mesoscale atmospheric models to study the impacts of wildfires at larger scale. Some of the topics on wildfire physical modelling that need further research are identified in the conclusions.

1. Introduction

Many factors have contributed to the increased wildfire hazard in Mediterranean regions (around the Mediterranean Basin, in the Iberian Peninsula, in southwestern USA and in Australia). One of the most critical factors was the rapid expansion of wildland–urban interface (WUI) and the reduction of agricultural activities (pastoral activity for example) that in the past contributed to landscape management. For example, in the USA in 2000, WUI covered around 9% of land area and contained

---

* Correspondence should be addressed to: Dominique Morvan, E-mail: dominique.morvan@univmed.fr

38% of all housing units [1]. In the context of global warming, one of the most moderate scenarios proposed by the Intergovernmental Panel on Climate Change (IPCC, B2: durable regional development) predicts, for summer in southern France in 2050, an average temperature increase of 2.9°C and a decrease of 38% and 15% in rainfall and groundwater (Météo France, http://climat.meteofrance.com/chgt_climat/accueil). Whatever the amplitude of global warming, this significant climate modification will contribute to increased fire hazard in these regions, with the repetition of catastrophic fire seasons, as observed in 2003 around the whole Mediterranean Basin, in 2007 in Greece and California, in 2008 in Australia and in 2009 in California [2].

The first paper describing, on physical bases, the mechanisms contributing to the propagation of surface fires was by Fons [3]. In that paper, he assimilated the propagation of fire as a succession of ignitions of adjacent pieces of fuel layer, playing successively the role of heat source and heat sink. In 1964, Emmons [4] was the first to propose a mathematical fire spread model, assuming that the main mechanism of heat transfer between the flame front and unburned vegetation was due to radiation. Later, works by Frandsen [5] and Rothermel [6] contributed to the development of one of the most widely used operational systems: BEHAVE. This model was based on a simple energy balance between the energy received by unburned fuel located ahead of the fire front and the energy necessary to sustain fire propagation (heat of vaporisation + heat of pyrolysis). In assuming that the rate of spread (ROS) of the fire front was constant, this energy balance equation was written in a reference frame attached to the fire front. To close the system, the energy flux received by the solid fuel was calculated as a fraction of the heat of combustion, and the constant of the model was evaluated empirically based on experimental fires, mainly carried out in a fire wind tunnel at the Intermountain Fire Science Laboratory (IFSL). Coupled with a geographical information system (GIS) describing the fuel structure and terrain slope at landscape scale, BEHAVE now constitutes the propagation model incorporated into the US operational system, FARSITE [7].

This class of model was referred to as empirical by Weber [8] in his review. In the same paper, he also introduced two other classes of models, namely statistical models and physical models. More recently, Sullivan provided a very detailed and interesting review concerning fire spread and fire behaviour models [9–11].

Practical use of semi-empirical models (such as BEHAVE or FARSITE) necessitates the definition of the vegetation structure using a finite set of fuel models [12]. The relative lack of success of this approach to reproduce correctly the behaviour of wildfires, especially in very heterogeneous fuel conditions, was very often attributed to the difficulty in defining an appropriate fuel model. Another source of uncertainties was also the domain of validity of parameters introduced to close the model, particularly the coefficient representing the fraction of energy received by the unburned vegetation in comparison with the energy released by the fire. This parameter was mainly evaluated empirically, using experimental fires carried out at small scale in a wind tunnel. In the absence of a real similitude analysis, extension of these results to large-scale fires is quite hazardous. In particular circumstances, this model can produce nonacceptable predictions, such as rate of spread larger than the wind speed [13, 14]. In semi-empirical wildfire models, the effects of wind and slope upon fire dynamics were treated in a similar

manner, considering that the main consequences of these external parameters were to modify the length and the trajectory of the flame, and consequently the radiative heat transfer between the flame and the vegetation. This approach is based on the assumption that the heat transfer between the flame and the solid fuel was mainly supported by radiation, which is far from reality, as indicated by Pitt [15] and Pagni and Peterson [16]. The role played by convective heat transfer, between the hot gases coming from the burning zone and pushed by the wind flow toward the vegetation located ahead of the fire front, is completely ignored.

Therefore, to improve knowledge of basic mechanisms governing the behaviour of wildfires, it appeared necessary to introduce more physics in a new generation of fire models [14, 17–19]. All these works can partially find their origin in the very interesting monograph proposed by Grishin [20] but also in other major contributions in this scientific field or more generally in fire modelling produced by many other authors such as Baum and McGrattan [21], Jones [22], Albini [23] and many others. This new class of wildfire models can be considered as a consequence of the rapid development, during these last decades, of computational fluid mechanics (CFD) tools in mechanical engineering, for the modelling of turbulent and reactive flows. The continual progress observed concerning computational power, concentrated on a personal computer or a cluster of computers, allowed simulation of very complex problems such as those encountered in a wildfire, i.e. degradation by drying and pyrolysis of vegetation, and the multiple interactions between turbulence and various phenomena such as combustion, drag force resulting from the presence of vegetation, radiative heat transfer and many other factors. This approach also allows the calculation of a huge number of variables (temperature of gas, temperature of solid fuel particles, heat fluxes received by convection and radiation by fuel particles, modifications of atmospheric flow induced by the fire etc.), which constitutes a valuable advantage (compared with other approaches) to understand in detail the roles played by various (possibly competing) physical mechanisms in the behaviour of wildfires.

2. Physical Mechanisms and Characteristics Length Scales Governing the Behaviour of Wildfires

In wildfires, two basic mechanisms contribute to heat transfer between the flame and the unburned vegetation: radiation coming from soot particles located in the flame, and convective heat transfer between the hot gases coming from the burning zone and vegetation located ahead of the fire front [16, 24]. The relative importance of these two heat transfer mechanisms depends on the competition between two forces: inertia due to wind flow, and buoyancy resulting from the density gradient between the hot plume above the fire and ambient air [25, 26]. The balance between these two contributions can be quantified by introducing the Byram convective number N_C, defined as the ratio between the rate of heat released from the fire and transferred vertically inside the plume versus the power of the inertial force due to the lateral wind flow [27–29]:

$$N_C = \frac{2gI_B}{\rho C_P T_0 (U_W - \text{ROS})^3}, \tag{1}$$

where g, ρ and C_P designate the acceleration of gravity, the density and the specific heat of the gas, and T_0 is the ambient temperature, respectively; U_W, I_B and ROS are the wind speed velocity, the fire line intensity and the rate of spread of the surface fire. The fire line intensity, I_B (kW/m), representing one of the most representative parameter of fire severity, can be evaluated using the Byram formula, as follows:

$$I_B = W \times H \times \text{ROS}, \tag{2}$$

using the following notation: W for weight of fuel consumed per unit area in the active flaming zone (kg/m^2), H for heat of combustion of solid fuel (kJ/kg) and ROS for rate of spread (m/s). Taking into account that part of the energy released by the fire is lost by radiation, the most usual value retained for H is 18,000 kJ/kg.

When $N_C \gg 1$, the behaviour of the fire is mainly governed by the dynamics of the thermal plume. In this case the trajectory of flames is nearly vertical and the convective column is well developed. The fire spread is mainly influenced by the fire itself and weakly by the wind. During propagation of the fire, one can observe strong updrafts characterised by rapid growth, followed by strong downdrafts after air is cooled in the upper part of the atmosphere. This phenomena promotes rapid descending air flow, which can caused collapse of the plume, with possible formation of a whirlwind. This fire configuration can promote high potential for spotting (more or less long-distance transport of burning particles, causing secondary ignition). This fire regime is referred to in the literature as plume dominated [30], and the heat transfer between the flames and vegetation is mainly supported by radiation.

When $N_C \ll 1$, the behaviour of fire is mainly controlled by wind flow. In this case, the thermal plume and flames are strongly deflected by the wind, and the variations of rate of spread are nearly linear in wind speed. This regime of fire propagation is referred to in the literature as wind driven [30], and propagation of the fire is mainly sustained by convective heat transfer; i.e. the hot gases coming from the burning zone are pushed by the wind flow, toward unburned fuel.

In considering the physical phenomena that lie at the origin of these two mechanisms of heat transfer, i.e. soot particles and the Stefan–Boltzmann σT^4 law for radiation, and local velocity magnitude and gas temperature T for convection, the second regime of propagation (namely wind-driven flow) is less affected by nonlinear mechanisms. Consequently, it is not surprising that the behaviour of such fires is more easily predictable, very often exhibiting linear dependence on wind speed velocity.

Because their behaviour are less predictable, plume-dominated fires are less studied experimentally. Nevertheless, this regime of fire propagation is also of great interest, to understand their erratic behaviour which can potentially cause

injuries to firefighters, during prescribed burning operation or suppression fire operations [26, 31].

To summarise, two mechanisms contributing to fire behaviour are clearly identified: wind flow, i.e. atmospheric boundary layer (ABL) flow, and radiative heat transfer between the flame and vegetation. These two physical phenomena can be characterised by two length scales: the turbulent integral length scale l_T for ABL and the extinction length δ_R characterising the penetration of radiative heat transfer inside the vegetation layer.

The roughness layer, representing the part of the ABL located between zero and three times the height of the canopy (H_{Fuel}), is mainly affected by coherent structures resulting from the shear interaction (Kelvin–Helmholtz instability), induced by the presence of the vegetation, with the wind flow. Consequently, l_T is strongly correlated with the height of the canopy ($l_T \approx H_{Fuel}$ horizontally and $l_T \approx H_{Fuel}/3$ vertically) [32–34]. Analyzing flow characteristics inside and just above the canopy, various authors noticed that the flow structure presented more similarities with a mixing layer than with a classical boundary layer flow. The transition between these two behaviours can be summarised using a product between two non-dimensional parameters: the drag coefficient C_D and the leaf area index (LAI), defined as the integration of the leaf area density (LAD $= \frac{\alpha_S \sigma_S}{2}$) through the whole canopy height. For $C_D \times \text{LAI} < 0.1$, the effects of drag inside the canopy are quite small and the turbulent boundary layer structure is maintained; above this threshold value, the flow changes toward a mixing layer regime [35, 47].

The extinction length scale δ_R is directly related to two physical characteristics of the vegetation layer: the surface-area-to-volume ratio σ_S and the packing ratio (i.e. the volume fraction occupied by the vegetation) α_S (Table 1):

$$\delta_R = \frac{4}{\alpha_S \, \sigma_S} = \frac{2 \times H_{Fuel}}{\text{LAI}}. \tag{3}$$

To calculate the radiation intensity field I (W/m^2/str) necessary to evaluate the radiative heat transfer, the following radiation transfer equation (RTE) must be solved [36]:

$$\frac{d\alpha_G I}{ds} = \alpha_G \sigma_a \left(\frac{\sigma T^4}{\pi} - I \right) + \sum_k \left[\frac{\sigma_S \alpha_S}{4} \left(\frac{\sigma T_S^4}{\pi} - I \right) \right]_k, \tag{4}$$

where the following notations are introduced: gas volume fraction α_G, gas + soot mixture extinction coefficient σ_a, temperature of the gas T and temperature of

Table 1
Typical values of attenuation length scale for various ecosystems

Fuel	Boreal forest	Mediterranean pine forest	Shrubs	Grass	Fuel bed
δ_R (m)	4.75	0.25	0.15	0.15–0.5	0.025

solid fuel particles T_S. The two terms on the right-hand side in Eq. 4, represent the contributions from the gas and the solid fuel particles (the k-summation is carried out over the whole set of solid fuel families) to the radiative heat transfer. The same terms (with opposite sign) must appear as source/sink terms in the energy balance equations for the gas mixture and the solid fuel particles.

To take into account temperature fluctuations due to atmospheric turbulent flow, the energy balance in the gas phase was treated using an averaging procedure. Using an optically thin fluctuation approximation (OTFA) [36], a term proportional to $\overline{T^4}$ appears in the radiative heat transfer term on the right-hand side of the average energy balance equation. The question is: how to evaluate this nonlinear term correctly? Can we simply use the following approximation: $\overline{T^4} \approx \overline{T}^4$? To answer this question, let us consider that the probability density function (pdf) affecting the fluctuation of temperature in the flame can be approximated using two Dirac distributions [$\delta(T - T_1)$ and $\delta(T - T_2)$], centred on two temperatures T_1 and T_2, respectively, equal to 500 K and 2,000 K [37, 38]:

$$\mathrm{pdf}(T) = 0.5\,\delta(T - T_1) + 0.5\,\delta(T - T_2). \tag{5}$$

Physically, using this expression we assume that the temperature of the gas oscillates equally between two temperature values T_1 and T_2. Using this approximation, it is straightforward to show that the ratio $\overline{T^4}/\overline{T}^4 \approx 3$, consequently it seems to be difficult to simulate correctly the radiative heat transfer coming from a fire when completely ignoring the turbulence/radiation interaction (TRI). Let us now consider another important subject concerning turbulent combustion modelling, especially the interaction between flames and turbulence. The large-scale structures that contain most of the turbulent kinetic energy of the flow have a size (the integral turbulence length scale) more or less equal to the depth of the vegetation layer. Assuming a wind velocity flow ranging between 5 and 10 m/s and a turbulence intensity (defined as the ratio between the root-mean-square turbulent velocity and the average velocity) ranging between 10% and 40%, we can evaluate roughly the scales of turbulence, as follows [39] (Table 2):

We know that the order of magnitude of the kinetic chemical time τ_C in a hydrocarbon flame is around 10^{-4} s [37, 40], which must be compared with the turbulence time scale, $\tau_T = l_T/K^{1/2}$ ($\sim$1 s), the ratio between these two quantities defined the Damköhler number $D_a = \tau_T/\tau_C$ ($\sim 10^4$). Considering that the slowest

Table 2
Rough estimations of some physical scales characterising the boundary layer flow above a canopy (grass, shrubs or trees)

Turbulence integral length scale l_T (m)	1–10 m
Velocity fluctuation (evaluated from TKE) $K^{1/2}$ (m/s)	0.5–10 m/s
Turbulent Reynolds number Re_T	3×10^4–2×10^6
Kolmogorov micro-length scale η (mm)	0.1–0.5

TKE turbulent kinetic energy.

phenomena of turbulence mixing and chemistry controls the time evolution of the combustion process, if fires are characterised by high Damköhler number, this means that the reaction rate is mainly controlled by the mixing process and very weakly by the kinetic process [40].

Let us now consider the physical phenomena occurring inside the vegetation layer and contributing also to the final behaviour of a propagating fire. First, it is necessary to define the level of detail necessary to describe the fuel complex layer. Except for some particular situations (homogeneous fuel bed or grassland for example), real vegetation, at landscape scale, is highly heterogeneous, being composed of various species, each structured by different solid fuel elements (foliage, twigs, trunk etc.). The question can be formulated as follows: how can one represent these very complex and heterogeneous structures? A part of the answer can be found in the physical properties characterising the vegetation and contributing effectively to the propagation of fires. These parameters are more or less identified: the fuel moisture content, the surface-area-to-volume ratio, the packing ratio (volume fraction) and the fuel density. Using this set of physical properties, it is possible to define classes (or families) of solid fuel particles representing the variability of fuel elements (foliage, twigs) composing a vegetation layer.

Experimental fires carried out in the laboratory (in dead fuel bed, on a flat terrain, without wind), propagating through homogeneous fuel beds, showed that the fire residence time (defined as the ratio between fire front depth and rate of spread: $\tau_{\text{Fire}} = \frac{L_{\text{Fire}}}{\text{ROS}}$) increased sharply when the thickness of the solid fuel particles exceeded 6 mm ($\sigma_S < 600 \text{ m}^{-1}$) (Table 3) [41]. Considering that the fire residence time reflects also the response time characterising each solid fuel elements composing a fuel complex when submitted to the thermal stress induced by a fire front, it seems reasonable to consider this value as a threshold for the finest fuel particles in the vegetation description (i.e. coarser fuel particles do not respond quickly enough to contribute actively to fire propagation). We can notice that this threshold coincides also with the 1-h fuel class used by foresters [30], corresponding to the part of the fuel which can reach an equilibrium state with ambient air in less than 1 h. In the field [42], many experimental observations have confirmed that the major part of fine fuel (90%) is consumed in the flaming zone and disappears after the transit of a surface fire.

Under the action of the thermal stress resulting from the heat released by the fire, the state of the vegetation located just ahead of the fire front exhibited the following evolution (see also Figure 1):

Table 3
Variations of fire residence time versus surface-area-to-volume ratio (fire propagating through a dead fuel bed, on a flat terrain, without wind)

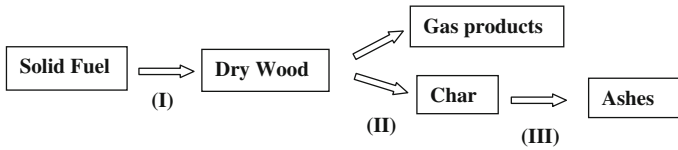| σ_S (m^{-1})	600	2000	5000	10000	20000
τ_{Fire} (s)	125	37	15	7	3

Figure 1. Mechanisms of thermal degradation of vegetation.

- If the local temperature exceeds a threshold value equal to 373 K, the foliage and the twigs dehydrate (step I);
- Between 400 K and 500 K, the dry solid fuel is subjected to a chemical reaction (pyrolysis) and is transformed into gas products (mainly CO, CO_2 and CH_4) and charcoal (step II);
- Above 700 K and under the action of ambient air, the surface of char is oxidized (step III).

To follow the evolution of the vegetation state, a set of solid fuel families representing the fuel complex were introduced in the model, each characterised using three mass fractions: water content, dry fuel and charcoal, complemented with a mass fraction representing residual ash.

3. Physical Modelling of Wildfires

In the rest of the text, we designate as a "fully" physical wildfire model a model based on the solution of the equations governing the evolution of the coupled system formed by the vegetation and the surrounding atmosphere. Models of this class are all based on a multiphase formulation. Of course, all physical scales cannot be directly calculated, as some of them (flame depth, Kolmogorov micro scale, individual fine fuel particles) must be simulated using a physical model. "Fully" physical wildfire models have seen a great development during the last decade. This approach was initially proposed by different authors [14, 19, 20, 43–46]. All these works were more or less based on the same basis. In introducing the term "fully physical model", we mean that the model must take into account the action of the wind flow upon the fire behaviour and also the retro-action of the fire itself upon the atmospheric flow. Considering this definition, we limited our review to four models developed from the references cited previously: FIRESTAR [a two-dimensional (2D) model developed at the University Aix-Marseille, UAM2], WFDS [a three-dimensional (3D) model developed at the Building and Fire Research Laboratory, BFRL-NIST], FIRETEC (another 3D model developed at Los Alamos National Laboratory, LANL) and FIRELES (a 3D model developed at the University of California Riverside). For these four tools, the evolution of the state of the coupled system formed by the vegetation and the surrounding atmosphere was calculated by solving two problems, the first one in the gas phase and the second one in the set of solid particles representing the vegetation.

The problem in the solid phase (vegetation) was formulated assuming that the vegetation stayed at rest and that the thickness of solid fuel particles was sufficiently small (<6 mm), and consequently that the energy balance equation can be solved assuming that the solid fuel particles can be considered as thermally thin (i.e. the temperature distribution inside each solid fuel particles can be considered as locally homogeneous). Two mechanisms of energy exchange with the gas mixture were introduced on the right-hand side of this equation: convective exchange between the hot or cold gas and the vegetation, and radiative heat transfer. Concerning the thermal degradation of solid fuel particles, the reaction rates reproducing the three steps described previously (drying, pyrolysis and surface oxidation) were evaluated using a Heaviside function for drying or two Arrhenius laws for pyrolysis and surface oxidation.

The problem in the gas phase was formulated by introducing two levels of averaging. A first one in space was introduced to homogenise the contribution resulting from the interaction between the vegetation and the wind flow. One consequence of this first step is the introduction of additional source/sink terms in the momentum and turbulence equations representing the average effect resulting from drag forces induced by the presence of solid fuel particles (foliage, branches, twigs) composing the vegetation. The second step, of time or space averaging, constituted the classical TRANS (Eq. 6c) or LES (Eq. 6d) filtering treatment. Using a mass average procedure (Favre), the continuity, momentum, turbulent (or sub-grid scale) kinetic energy, energy and chemical species balance equations can be written as follows:

$$\frac{\mathrm{D}\bar{\rho}}{\mathrm{D}t} = \sum_{\alpha} \bar{M}_{\alpha}^{(\mathrm{S})} \tag{6a}$$

$$\frac{\mathrm{D}\bar{\rho}\tilde{u}_i}{\mathrm{D}t} = \frac{\partial(\overline{\alpha_\mathrm{g}\sigma_{ij}})}{\partial x_j} - \frac{\partial}{\partial x_j}(\overline{u_j''u_i''}) + \bar{\rho}g_i - \rho C_\mathrm{D}\frac{\alpha_\mathrm{S}\sigma_\mathrm{S}}{2}\|\tilde{U}\|\tilde{u}_i \tag{6b}$$

$$\frac{\mathrm{D}\bar{\rho}K}{\mathrm{D}t} = \frac{\partial}{\partial x_j}\left(\frac{\mu_\mathrm{eff}}{\sigma_K}\frac{\partial K}{\partial x_j}\right) + \bar{\rho}P - \bar{\rho}\varepsilon + \rho C_\mathrm{D}\frac{\alpha_\mathrm{S}\sigma_\mathrm{S}}{2}\|\tilde{U}\|\left(\|\tilde{U}\|^2 - \beta_\mathrm{D}K\right) \quad 1 \le \beta_D \le 5 \tag{6c}$$

$$\frac{\mathrm{D}\bar{\rho}K}{\mathrm{D}t} = \frac{\partial}{\partial x_j}\left(\frac{\mu_\mathrm{eff}}{\sigma_K}\frac{\partial K}{\partial x_j}\right) + \bar{\rho}P - \bar{\rho}C_\varepsilon\frac{K^{3/2}}{L_\mathrm{SGS}} - 2\rho C_D\frac{\alpha_\mathrm{S}\sigma_\mathrm{S}}{2}\|\tilde{U}\|K \quad C_\varepsilon = 0.93 \tag{6d}$$

$$\frac{\mathrm{D}\bar{\rho}\tilde{h}}{\mathrm{D}t} = \frac{\partial\overline{q_j}}{\partial x_j} - \frac{\partial}{\partial x_j}(\overline{u_j''h''}) - \overline{Q_\mathrm{CONV}^{(\mathrm{S})}} \tag{6e}$$

$$\frac{\mathrm{D}\bar{\rho}\tilde{Y}_\alpha}{\mathrm{D}t} = \frac{\partial}{\partial x_j}\left(\rho D \frac{\partial \tilde{Y}_\alpha}{\partial x_j}\right) - \frac{\partial}{\partial x_j}(\overline{u_j'' Y_\alpha''}) + \overline{W_\alpha} + \overline{M_\alpha^{(\mathrm{S})}}, \tag{6f}$$

using the following notation:

ρ Bulk density of the gas phase ($\rho = \alpha_g \rho_g$)

α_g Volume fraction of the gas phase

α_S Volume fraction of the solid phase (vegetation)

u_i i-th component of the velocity vector

σ_S Average value of surface-area-to-volume fraction (SA/V) of solid fuel particles representing the vegetation $\alpha_S \sigma_S = \sum \alpha_S^K \sigma_S^K$ (α_S^K and σ_S^K designate, respectively, the volume fraction and the SA/V attached to one family of solid fuel particles)

σ_{ij} Stress tensor

g_i Acceleration of gravitation

h Enthalpy

q_j Heat flux (molecular diffusion and radiation)

Y_α Mass fraction of chemical species

T Gas temperature

μ Dynamical viscosity

K Turbulent kinetic energy (TKE)

All last terms on the right-hand side of these equations represent the additional terms coming from the interaction between ambient atmosphere and vegetation (gas production due to pyrolysis reaction, drag force, heat transfer by convective exchange etc.). Concerning the effects of drag force upon the turbulence budget (Eq. 6c and Eq. 6d), the source term (proportional to U^3) represents the production of wake turbulence due to the presence of branches, twigs and foliage inside the canopy. The sink term (proportional to $U \times K$) represents the rapid dissipation of turbulence by short-circuiting of the Kolmogorov cascade [47].

Concerning the treatment of turbulence, various approaches were proposed, from TRANS (FIRESTAR, http://www.eufirestar.org, [25, 26]), multi-scale LES (FIRETEC, [18] and LES (WFDS, [14, 46], FIRELES, [19, 48]).

Concerning the resolution of the radiation transfer equation (RTE), comparable approaches were used in FIRESTAR, FIRELES and WFDS: discrete ordinate method (FIRESTAR, FIRELES) and finite volume method (WFDS) [36]. The main advantage of this method is that it is well adapted to a large range of optical thickness, defined as the product of the extinction coefficient with a typical length scale. As underlined in previous part, fires are subjected to large temperature fluctuations (especially in the gas phase) and consequently turbulence and radiative heat transfer interact strongly each other. Only FIRESTAR takes this phenomena into account directly in the energy balance equation and in the RTE. Assuming that the turbulent optical thickness, defined as the product of the extinction coefficient in the gas with the integral turbulent length scale ($\sigma_a \times l_T$), is small, the correlation between the extinction coefficient and the radiation intensity can be neglected (optically thin fluctuation approximation,

OTFA) and the average radiation transfer equation (RTE) can written as follows [49]:

$$\frac{d\alpha_G \bar{I}}{ds} = \alpha_G \left(\frac{\sigma \overline{\sigma_a T^4}}{\pi} - \overline{\sigma_a} \bar{I} \right) + \sum_k \left[\frac{\sigma_S \alpha_S}{4} \left(\frac{\sigma T_S^4}{\pi} - \bar{I} \right) \right]_k . \tag{7}$$

On the right-hand side of Eq. 7, the non-linear term $\overline{\sigma_a T^4}$ can be approximated as follows (assuming that the pdfs of fluctuating variables are Gaussian, and that correlations of odd order are identically zero):

$$\overline{\sigma_a T^4} \approx \overline{\sigma_a} \overline{T}^4 \left[1 + 6\frac{\overline{T'^2}}{\overline{T}^2} + \frac{\overline{T'^4}}{\overline{T}^4} + 4\frac{\overline{\sigma'_a T'}}{\overline{\sigma_a} \overline{T}} + 4\frac{\overline{\sigma'_a T'^3}}{\overline{\sigma_a} \overline{T}^3} \right]. \tag{8}$$

Experimental data showed that $\overline{T'^4}/\overline{T}^4 \ll 6\overline{T'^2}/\overline{T}^2$, and as a first approximation the fluctuations of extinction coefficient can be neglected. Using this approximation, to solve the TRI problem, it is necessary to introduce an additional variable, representing the variance of the temperature field: $\overline{T'^2}$ [50, 51]. Because TRI modelling needs to represent phenomena at a relative small scale (formally, the mesh size δ in the vegetation layer must be smaller than the extinction length scale δ_R), the radiative heat transfer in WFDS was evaluated in such a manner, i.e. that it cannot be smaller than a fraction of the heat of combustion heat release rate, introducing an empirical ratio ranging between 0.2 and 0.4. In FIRETEC, the radiative heat transfer was treated differently, using a modified diffusion method. Theoretically the diffusion method (also called the P1-approximation) to solve RTE is adapted to relatively optically thick medium (i.e. medium characterised by optical thickness larger than 1). In the region located between the flame and the top of the unburned vegetation layer, where accurate evaluation of radiation is crucial, the medium can be considered as quasi-transparent, and in this case the use of a diffusion model to solve RTE can be completely inappropriate. When convection constitutes the main heat transfer mechanism controlling the propagation of fire (wind-driven fire), this failure to calculate the radiative heat transfer correctly does not have great consequences. When radiative heat transfer can play an important role in the behaviour of fire (plume-dominated fire, ignition of the base of a canopy from a surface fire etc.), use of such an approach can be more problematic. Conscious of this problem, the team in charge of the development of FIRETEC is implementing a new radiation module, based on a Monte-Carlo approach [36]. Concerning the TRI in FIRETEC, this was partially taken into account by multiplying all the contributions of the form T^4 (i.e. $\overline{T^4} \approx k\overline{T}^4$) by a factor $k > 1$. No particular treatment concerning TRI was reported in FIRELES.

Concerning the chemical problem in the turbulent flame, based on experimental analysis [20] the composition of pyrolysis products in FIRESTAR and FIRELES was limited to a $CO + CO_2$ mix, reducing the chemical kinetics in the combustion zone to:

$$CO + 0.5 O_2 \rightarrow CO_2. \tag{9}$$

In WFDS, the composition of the pyrolysis was chosen as more complex:

$$C_{3.4}H_{6.2}O_{2.5} + 3.7\,O_2 \rightarrow 3.4\,CO_2 + 3.1\,H_2O. \tag{10}$$
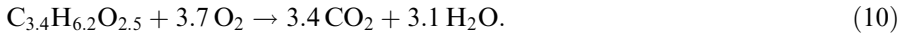
In all models (FIRESTAR, FIRELES and WFDS), the combustion reaction rate was calculated using an EDC model, assuming that the turbulent mixing process constituted the main physical phenomena limiting the reaction rate (see the previous discussion concerning the Damköhler number) [26, 46, 52, 53].

In FIRETEC, transport of chemical species was not directly calculated. Because this tool was initially dedicated to simulate wildfires at relative large scale, using a relatively coarse grid (mesh size not smaller than 1 m), consequently pyrolysis and combustion phase were assumed to take place at the same location (without transport and mixing phase). This approach consists of reducing the pyrolysis and the gaseous combustion processes, using a single-step heterogeneous combustion schema, as follows (written here in mass):

$$\text{Solid\_Fuel} + N_S\,O_2 \rightarrow (1 + N_S)\text{Products}, \tag{11}$$
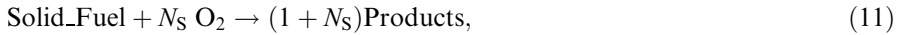
where N_S is the stoichiometric coefficient (mass of oxygen necessary to burn 1 kg solid fuel).

Consequently the heat release rate (HRR) was directly calculated from the fraction of burning solid fuel, evaluated from the temperature (average + presumed distribution) in the solid fuel and the average mass fraction of oxygen. Recently a sub-grid mixture fraction-based thermodynamic equilibrium model was also introduced in FIRETEC for the gas-phase combustion [54].

The formulations of the flow problem used in the four models were not all similar: FIRESTAR was based on an implicit solver, while FIRETEC, FIRELES and WFDS were based on explicit solver [certainly to reduce central processing unit (CPU) time and to simplify code development].

Concerning the density/pressure/velocity coupling, FIRESTAR, FIRELES and WFDS are both formulated using a low-Mach-number approximation, while FIRETEC uses a fully compressible formulation. Considering the CFL limitation attached to explicit formulations, this choice (fully compressible/low Mach) has a large effect on the numerical efficiency of these models [55]; i.e. for subsonic flow, a simulation carried out using a fully compressible formulation needs to solve the problem using a time step significantly smaller than the same simulation performed using a low-Mach-number approximation, the ratio between the two time steps being approximately equal to the Mach number:

$$\frac{\Delta t(\text{Full compressible})}{\Delta t(\text{Low Mach})} = \text{Mach}. \tag{12}$$

Concerning the representation of real fuel complex (fully heterogeneous vegetation), FIRESTAR, FIRELES, WFDS and FIRETEC are all able to take into account the presence of various solid fuel particles types inside the same grid cell, representing the local variability in size (surface-area-to-volume ratio) and state

(moisture content, density) inside the vegetation layer. This characteristic is particularly interesting for studying the interaction between dead and living fuel, as occurs for a fire propagating in a fully heterogeneous fuel complex (such as in chaparral) or for studying surface-to-crown fire transition in forest fires.

The mesh size Δ used to represent numerically the physical domain cannot be chosen without taking into account some physical considerations. Keeping in mind than both the ABL/canopy turbulence and the radiative heat transfer play an important role in propagation of fires, Δ must at least satisfy the following constraint:

$$\Delta < \min\left(\frac{H_{\text{Fuel}}}{3}, \frac{2\,H_{\text{Fuel}}}{\text{LAI}}\right). \tag{13}$$

If this criteria cannot always be verified, mainly for CPU time reasons (3D calculations), it must be compensated by introducing a sub-grid model. This is the case, for example in WFDS, when the surface fuel cannot be fully represented for large-scale simulations and is replaced by a "boundary fuel element" option (the energy balance inside the surface fuel layer is treated separately and the result of this sub-model is then introduced as source terms in the problem concerning the gaseous phase). Of course in this case, a part of the physics is lost (here the details of the flow inside the surface fuel layer are not fully reproduced), but this is certainly the price to pay for solving such problems in reasonable CPU time.

In Table 4 we have summarised, for the four codes reported herein, the main physical and numerical properties characterising each of them. Each model has its own set of characteristics. At this stage it is difficult to compare all these models directly. Some comparisons have been proposed based on benchmarks carried out for surface fire propagating through grassland [55], indicating that WFDS is more efficient in terms of computational time compared with FIRETEC (this result is certainly due to the low-Mach-number formulation used in WFDS and also to the very efficient Poisson solver used to calculate the pressure correction). Concerning accuracy, it is more difficult to determine the more accurate model. Too many non-linear phenomena (turbulence, combustion, radiation) can contribute to the final behaviour of fires. This question can only be treated for experimental fires at small scale, in well-controlled conditions [46, 56].

Table 4
Summary of the main characteristics of four fully physical fire models

	Numerical	Low Mach model	Turbulence	TRI model	Combustion model	Multi-fuel model	Low scale	Large scale
FIRESTAR	2D implicit	Yes	TRANS	Yes	Yes	Yes	Yes	Yes[***]
WFDS	3D explicit	Yes	LES	Yes[*]	Yes	Yes	Yes	Yes
FIRETEC	3D explicit	No	LES	Yes[*]	No[**]	Yes	No	Yes
FIRELES	3D explicit	Yes	LES	No	Yes	No	Yes	No

* Radiative heat transfer increased empirically.
** Pyrolysis and combustion take place at the same location without a transport phase.
*** With the limitation introduced by the 2D assumption.

4. Results and Discussion

We now illustrate some capabilities offered by these four codes (FIRESTAR, FIRELES, WFDS and FIRETEC), to reproduce some physical behaviours of fires at various scales.

Experimental fires [57] carried out in a wind tunnel at the Intermountain Fire Science Laboratory, using various homogeneous fuel beds (pine needles, excelsior, wood sticks), constitute one of the most significant experimental databases to test physical fire models at small scale. One of the main advantages of using these experimental data is that the conditions of propagation of fires were well characterised (flow in wind tunnel, composition and state of solid fuel bed), which is far from the case for outdoor experimental fires. Due to limitations in grid size in FIRETEC (pyrolysis and combustion took place at the same location), this configuration was only tested using FIRESTAR and WFDS models. In Figure 2 we can see the results obtained using FIRESTAR. At the top we can see a typical temperature field obtained for a simulation carried out in a pine needles fuel bed.
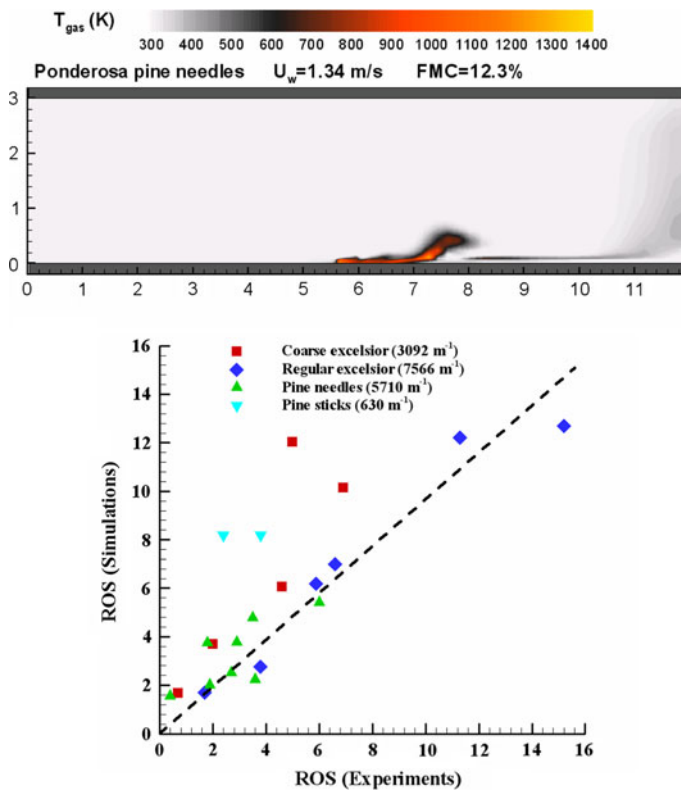
Figure 2. Simulation of a surface fire propagating in a pine needles fuel bed (*top*), and simulated rate of spread (ROS) versus experimental ROS (*bottom*) (FIRESTAR results).

Even if the wind flow was relatively moderate (U_W = 1.34 m/s), the trajectory of the flame was significantly deviated along the streamwise direction. At the bottom is presented the rate of spread (ROS) of fires, evaluated from the trajectory of the isotherm T = 500 K in the solid fuel (representing more or less the position of the pyrolysis front), versus the ROS measured experimentally. Taking into account the fact that the behaviour of fires was governed by combined effects of various non-linear processes (decomposition by pyrolysis of solid fuel, turbulent flow and mixing process between pyrolysis products and air, radiative heat transfer etc.), we can consider that the agreement between experimental and numerical predictions concerning ROS is not so bad. Many points were located near the diagonal axis (representing the ideal case), and the worst results were obtained with pine sticks, characterised by a surface-area-to-volume ratio of 630 m^{-1}, corresponding to the limit of validity of the thermally thin assumption used for solid fuel to solve the energy balance equation.

Another comparison at small scale was proposed using WFDS, for an experimental fire carried out in a single, tall ($\sim$2 m high) Douglas fir at the Building and Fire Research Laboratory (BFRL-NIST) [46]. The experiments were performed for various fuel (needles) moisture content, ranging from 10% to 50%. As shown in Figure 3, the dynamics of the two fires (experimental and simulated) were quite similar. The curves representing the time histories of mass loss rates and incident radiant heat fluxes (obtained numerically) compared fairly well with experimental data measured in similar conditions [46] (both in amplitude and in dynamics), confirming that the agreement between experimental and numerical results was not only qualitative but also quantitative. Concerning the representation of fuel, two options were implemented in WFDS: 'Fuel element model' including all the interaction terms between ABL and vegetation (this option was used in the example described previously and in [46], and 'Boundary fuel element
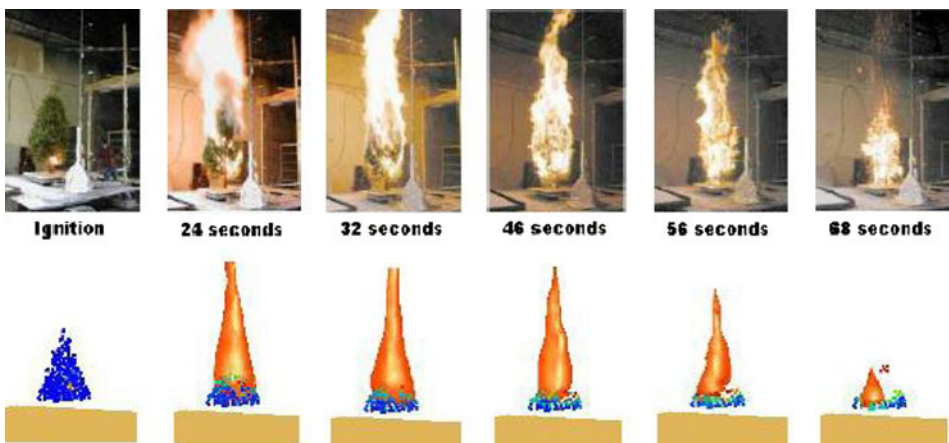

Figure 3. **Experimental fire and simulation (using WFDS) carried out in a tall Douglas fir (courtesy of W. Mell from BFRL-NIST) [46].**
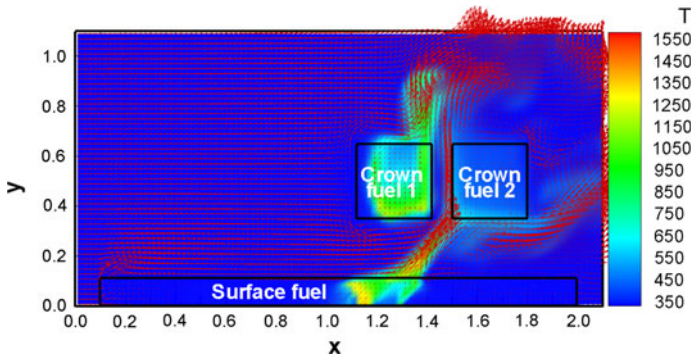
Figure 4.   Large-eddy simulation of surface-to-crown fire transition in shrubs carried out in 3D using FIRELES: temperature field and velocity vectors (private communication from J. Lozano, S. Mahalingam and D. Weise).

model', for which the surface fuel was represented as an homogeneous solid fuel layer treated in a separate calculation [14]. This simplified description was developed to facilitate (by reducing constraints on the grid size), the use of WFDS at very large scale and when most of the active combustion takes place in the gas phase above the vegetation.

Other experimental configurations have also been tested to compare "fully" physical wildland fire models with real fires; we can reported for example the works [19, 48], both carried out using FIRELES. The temperature field and the velocity vectors obtained at a midplane, to simulate the surface-to-crown fire transition (at small scale), are shown in Figure 4. For this calculation, the fuel complex was composed of shrubs (chamise, fuel moisture content ranged between 36% and 53%) and excelsior on the ground (FMC less than 10%).

As indicated above, pyrolysis and gaseous combustion were assumed to occur at the same place in FIRETEC; consequently, even if the mesh size can theoretically be reduced, FIRETEC is not appropriate to simulate fires at small scale.

The experimental campaigns carried out in the Northern Territory in Australia [58–60] certainly constitute one of the most interesting databases published to study fires at large scale. These results were widely used by all teams developing wildfires models on physical bases [14, 26, 31, 61].

These experimental fires were conducted on a flat terrain with quite homogeneous vegetation (grass), well characterised physically (height, fuel load, surface-area-to-volume ratio, fuel moisture content), and the external flow conditions (i.e. the 2 m or 10 m open wind velocity) were relatively well known. To illustrate what can be done for this kind of configuration, the temperature field (gas) and the velocity vectors simulated using FIRESTAR for a 10 m open wind velocity U_{10} equal to 3.9 m/s are shown in Figure 5. This result clearly highlights the barrier formed by the plume above the burning zone, separating the flow into two zones: windward dominated by the inlet wind flow deviated vertically by the
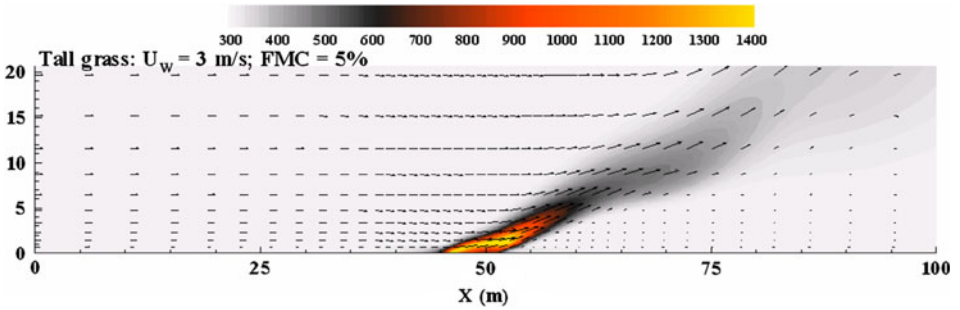
Figure 5. Example of fire simulation (temperature and velocity vectors) of surface fire propagating in grassland, using FIRESTAR (U_{10} = 3.9 m/s).

plume, leeward mainly affected by the presence of the fire where the streamwise velocity component can be negative (in-draft flow). We cannot fully exclude the possibility that such phenomena can be artificially enhanced in 2D simulations, because of the impossibility for the flow to bypass the flame front. The rate of spread (ROS) versus the 10 m open wind velocity (U_{10}) is shown in Figure 6. On the same plot, we also present results obtained using FIRESTAR (in 2D) and
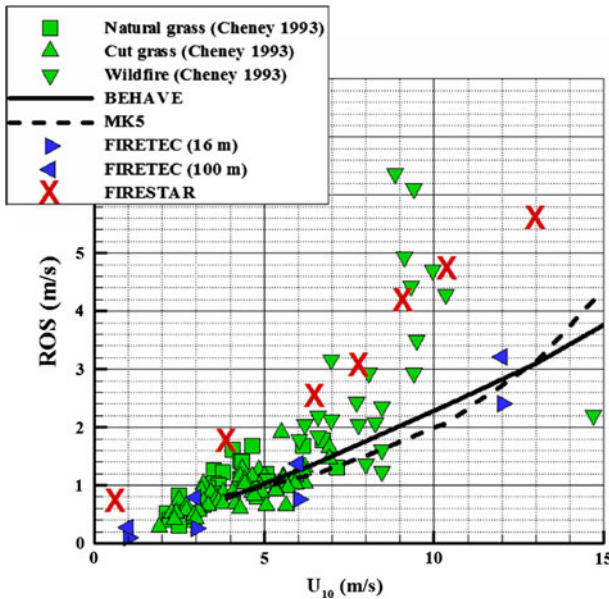

Figure 6. Rate of spread (ROS) versus 10 m open wind velocity (U_{10}) obtained in tall grass using FIRESTAR and FIRETEC, compared with experimental observations [59] and predictions using empirical operational models BEHAVE [66] and MK5 [62].

FIRETEC (in 3D); we have also added predictions obtained using two operational empirical (MKV) and semi-empirical (BEHAVE_PLUS) models [62, 66]. The numerical simulations (FIRESTAR and FIRETEC) were carried out using exactly the same fuel properties corresponding to tall grass: fuel load 7 t/ha, fuel depth 0.7 m, SA/V 4000 m^{-1} and FMC 5%. On the same curve, the symbols represent observations and measurements carried out on experimental fires and bushfires [58]. The simulations performed in 3D were done for two values of initial head fire width L_{ign} (16 and 100 m) to illustrate the influence of this parameter upon the ROS. As previously shown experimentally [59], the ROS was significantly affected if the head fire width was smaller than 50 m, before reaching an asymptotic value for $L_{ign} > 100$–150 m. Because FIRESTAR simulations were carried out in 2D, in this case the head fire width was assumed to be infinitively long. The results obtained in 3D using FIRETEC partially reflected this phenomena; however, it seems that the increase of the ROS was less pronounced for numerical simulations [ROS(100 m)/ROS(16 m) ≈ 1.33] than experimentally [ROS(100 m)/ROS(16 m) ≈ 2.12]. We can also mention that the same test was also carried out using WFDS and reported in [14]. In these simulations the spread rate of head fire was well predicted in the range of wind speeds considered. A detailed analysis of the spread of the entire fire line was also compared with two experimental Australian fires, exhibiting reasonably good agreement. We can notice on this curve the trend followed by empirical models (BEHAVE and MK5) for relatively strong wind conditions (>10 m/s), systematically (in this case) under-predicting the ROS compared with values observed in the field [13].

This defect was already underlined in the literature; it is a direct consequence of the range of experimental data used to calibrate the empirical constants integrated in these models. For practical and safety reasons, all experimental fires were conducted at small scale and/or for moderate wind conditions. The defects highlighted by empirical models were at the origin for the development of a new class of models based on more physical approach. Of course, the evolution from empirical to "fully" physical models promoted a considerable increase of the level of complexity, excluding for the moment the application of this new class of models in the same conditions currently used for empirical models. We can consider that the use of "fully" physical models can be reserved to improve knowledge concerning the physics of fires, to identify and quantity the physical mechanisms of propagation and to study the impact of fires on potential target (in the wildland–urban interface, for example).

To simulate experimental fires or wildland fires propagating in fully heterogeneous fuel layer (such as chaparral), it is necessary to represent in more detail the structure of the vegetation by introducing a set of solid fuel families for each solid fuel elements such as foliage, twigs and branches present inside the fuel layer, in two states (dead and alive). Actually this modelling approach was already done in FIRELES, WFDS and FIRESTAR (preliminary work was also recently presented for FIRETEC [63]). Figure 7 presents the temperature field and velocity vectors, simulated using FIRESTAR, in conditions similar to an experimental fire carried out in a Mediterranean maquis (the experiment was performed in Galicia, northwestern Spain). To represent the vegetation layer (1.25 m high, mainly composed of *Ulex europaeus* and *Ulex minor*), we used 14 solid fuel families, and the fuel
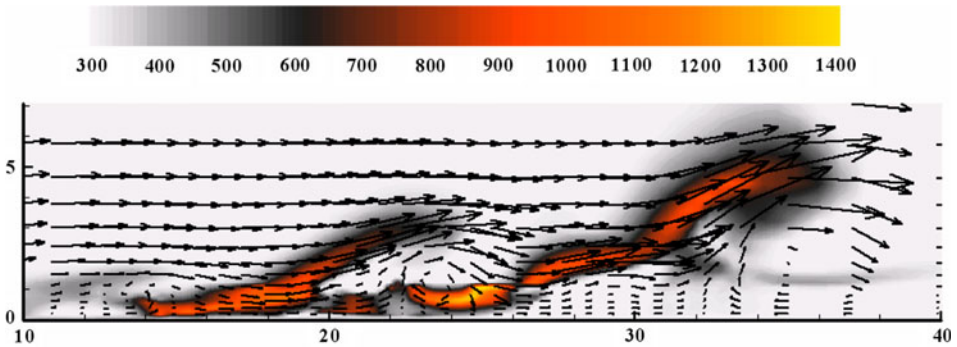
Figure 7.   Numerical simulation (FIRESTAR) of a wind-driven fire propagating in Mediterranean shrubland (maquis).

moisture content ranged from 108% to 150% (living fuel) and from 10% to 32% (dead fuel). The slope of the terrain was 5%, and the average open wind speed, U_{10}, was measured as 5.7 m/s. This snapshot (Figure 7) clearly highlights how convective heat transfer can contribute to the propagation of the fire, in promoting recirculation of hot gases ahead of the fire front. For this simulation we found a rate of spread (ROS), evaluated using the trajectory of the isotherm T_S = 500 K (in the solid fuel), equal to 0.248 m/s, compared with ROS = 0.273 m/s observed during the experiment.

Extension of this class of fire model to relatively large-scale configurations, studying the behaviour and effects of fires upon structures in wildland–urban interface (WUI), is underway. This issue can be considered as particularly important, considering the surfaces concerned and the number of habitation units located in the WUI [1]. One of the most advanced tools to study this problem seems to be WFDS (in fact, all the specific models initially developed for WFDS have now been implemented in FDS: Fire Dynamics Simulator; http://fire.nist.gov/fds/). The result shown in Figure 8 illustrates a simulation carried out for a surface fire propagating through a WUI community. For this calculation, the dimensions of the domain were 240 m × 240 m horizontally and 100 m vertically. In addition to the representation of the fire front, walls and roofs are coloured according to the potential impact of incident heat flux upon the state of materials constituting these different elements of habitation units. Upscaling of the physical fire models to larger domains (8 km × 8 km) is also in progress (private communication), potentially including connection between physical fire models at fine scale with nonhydrostatic, mesoscale atmospheric models (such as WRF).

This new scientific frontier, concerning wildfire modelling, can be considered as highly strategic, to quantify the emissions of wildfires (green gases, aerosols, smoke etc.) and their impacts on carbon cycle and global warming, risks to health and micro-meteorology.
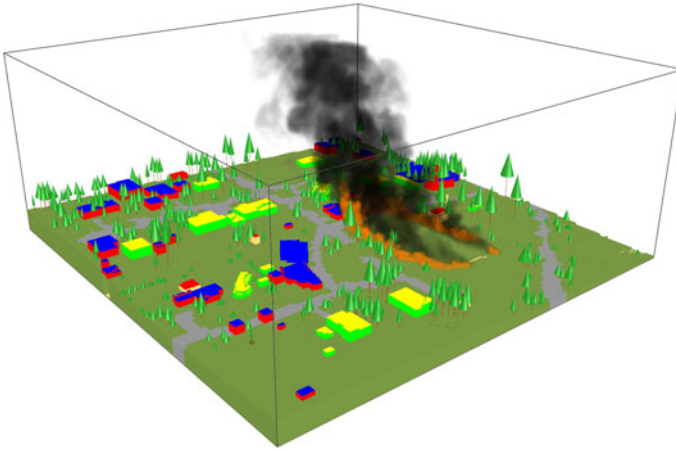
Figure 8.   Numerical simulation (WFDS) of a surface fire propagating through a WUI community (walls and roofs coloured according to fire safety criteria) (private communication from W.E. Mell).

Figure 9.   Aerial view of a wildfire.

   To improve upscaling and develop a real-time fire simulator, it is necessary to apply some compromises concerning the description of the fire, reducing the fire front as a heat release zone propagating on a GIS surface. As shown in Figure 9, representing an aerial view of a wildfire, at a certain scale, a fire front can be considered as a thick line separating the ground surface into two regions: burned and unburned area. Following this approach, two physical models, coupled with a nonhydrostatic mesoscale atmospheric models (WRF or MESONH), were recently proposed [64, 65].

5. Conclusions

During the last decade, "fully" physical approaches to study the behaviour of wildland fires have seen considerable development. Despite the very complex nature of physical phenomena involved in ignition, development and propagation of natural fires (atmospheric turbulence, pyrolysis and combustion reactions, radiative heat transfer etc.), this approach has proved its ability to reproduce many of these physical phenomena such as: The existence of two basic regimes of propagation (wind driven and plume dominated) characterising surface fires was clearly identified and characterised in terms of heat transfer (the role played by radiation and convection was quantified); The transition of surface fires to ignite a canopy can also be reproduced; The differences of behaviour between head fire and backfire were correctly simulated, along with many other physical phenomena. Considering very recent works presented on this subject, there is also great interest in use of this approach to study the behaviour of surface fires propagating through a WUI, in order to reduce fire hazard and the impacts on communities living in these urban areas. The emission of wildfires (greenhouse gases, aerosols) will also be more accurately quantifiable in the future, by coupling "fully" physical models or simplified physical models with mesoscale atmospheric models.

Acknowledgment

References

1. Radeloff VC, Hammer RB, Stewart SI, Fried JS, Holcomb SS, McKeefry JF (2005) The wildland-urban interface in the United States. Ecol Appl 15(3):799–805
2. Mell WE, Manzello SL, Maranghides A, Butry D, Rehm RG (2010) The wildland-urban interface fire problem current approaches and research needs. Int J Wildland Fire (in press)
3. Fons WL (1946) Analysis of fire spread in light forest fuels. J Agri Res 72(3):93–121
4. Emmons H (1964) Fire in the forest. Fire Res Abstr Rev 5:163–178
5. Frandsen WH (1971) Fire spread through porous fuels from the conservation of energy. Combust Flame 16:9–16
6. Rothermel R (1972) A matrhematical model for predicting fire spread in wildland fuels. Technical report, USDA Forest Service Research, INT-115
7. Finney MA (1998) FARSITE: fire area simulator, model development and evaluation. USDA-Forest Service Research, INT-4
8. Weber RO (1991) Modelling fire spread through fuel beds. Prog Energy Combust Sci 17:67–82
9. Sullivan AL (2009) Wildland surface fire spread modelling 1990–2007: 1 physical and quasi-physical models. Int J Wildland Fire 18(4):349–368

10. Sullivan AL (2009) Wildland surface fire spread modelling 1990–2007: 2 empirical and quasi-empirical models. Int J Wildland Fire 18(4):369–386
11. Sullivan AL (2009) Wildland surface fire spread modelling 1990–2007: 3 simulation and mathematical analog models. Int J Wildland Fire 18(4):387–403
12. Scott JH, Burgan RE (2005) Standard fire behavior fuel models: a comprehensive set for use with Rothermel's surface fire spread model. USDA-Forest Service Research Report RMRS-GTR-153
13. Hanson HP, Bradley MM, Bossert JE, Linn RR (2000) The potential and promise of physics-based wildfire simulation. Environ Sci Policy 3:161–172
14. Mell W, Jenkins MA, Gould J, Cheney Ph (2007) A physics-based approach to modelling grassland fires. Int J Wildland Fire 16(1):1–22
15. Pitts WM (1991) Wind effects on fires. Prog Energy Combust Sci 17:83–134
16. Pagny PJ, Peterson TG (1973) Flame spread through porous fuel. Proc Combust Instit 14:1099–1107
17. Morvan D, Dupuy JL (2004) Modelling the propagation of a wildfire through a Mediterranean shrub using a multiphase formulation. Combust Flame 138:199–210
18. Linn RR, Reisner J, Colman JJ, Winterkamp J (2002) Studying wildfire behaviour using FIRETEC. Int J Wildland Fire 11:233–246
19. Zhou X, Mahalingam S, Weise D (2007) Experimental study and large eddy simulation of effect of terrain slope on marginal burning in shrub fuel beds. Proc Combust Instit 31:2547–2555
20. Grishin AM (1997) In: Albini F (Ed) Mathematical modelling of forest fires and new methods of fighting them. Tomsk State University, Tomsk
21. Baum HR, McGrattan KB (2000) Simulation of large industrial outdoor fires. In Fire Safety Science. In: Proceedings of the sixth international symposium. International Association for Fire Safety Science
22. Jones WP (1994) Turbulence modelling and numerical solution methods for variables density and combusting flows. In: Libby PA, Williams FA (eds) Turbulent reacting flows, vol 6. Academic, London, pp 309–374
23. Albini FA (1981) A model for the wind-blown flame from a line fire. Combust Flame 43:155–174
24. Whelan RJ (1995) The ecoly of fire. Cambridge University Press, Cambridge
25. Morvan D, Méradji S, Accary G (2008) Wildfire behavior study in a Mediterranean pine stand using a physically based model. Combust Sci Tech 180(2):230–248
26. Morvan D, Méradji S, Accary G (2009) Physical modelling of fire spread in Grasslands. Fire Safety J 44:50–61
27. Byram G (1959) In: Davis K (Ed) Forest fire control and use. McGraw-Hill, New York, pp 90–123
28. Nelson RM (1993) Byram's derivation of the energy criterion for forest and wildland fires. Int J Wildland Fire 3(3):131–138
29. Sullivan AL (2007) Convective Froude number and Byram's energy criterion of Australian experimental grassland fires. Proc Combust Instit 31:2557–2564
30. Pyne SJ, Adrews PL, Laven RD (1996) Introduction to wildland fire, 2nd edn. Wiley, New York
31. Morvan D, Hoffman Ch, Rego F (2009) Numerical simulation of the interaction between two fire fronts in the context of suppression fire operations. In: 8th Symposium on fire and forest meteorology, Kalispell, MT-USA, 13–14 October 2009
32. Finnigan JJ (2000) Turbulence in plant canopies. Ann Rev Fluid Mech 32:519–571
33. Kaimal JC, Finnigan JJ (1994) Atmospheric boundary layer flows. Oxford University Press, Oxford

34. Raupach MR, Thom AS (1981) Turbulence in and above plant canopies. Annual Rev Fluid Mech 13:97–129
35. Ghisalberti M, Nepf H (2006) The structure of the shear layer in flows over rigid and flexible canopies. Environ Fluid Mech 6:277–301
36. Modest MF (2003) Radiative heat transfer, 2nd edn. Academic, London
37. Warnatz J, Maas U, Dibble RW (1999) Combustion: physical and chemical fundamentals, modeling and simulation, experiments, pollutant formation, 2nd edn. Springer, Berlin
38. Cox G (1996) Combustion fundamentals of fire, 2nd edn. Academic, London
39. Pope SB (2000) Turbulent flows. Cambridge University Press, Cambridge
40. Borghi R, Champion M (2000) Modélisation et théorie des flammes, TECHNIP edn
41. Burrows ND (2001) Flame residence times and rates of weight loss of eucalypt forest fuel particles. Int J Wildland Fire 10:137–143
42. Cheney NP (1981) In: Gill RH, Groves RH, Noble IR (eds) Fire and the Australian biota. Autralian Academy of Science, Canberra, p 151
43. Linn RR (1997) A transport model for prediction of wildfire behaviour. PhD thesis University of New Mexico, LANL
44. Larini M, Giroud F, Porterie B, Loraud JC (1998) A multiphase formulation for fire propagation in heterogeneous combustible media. Int J Heat Mass Transf 41(6–7):881–897
45. Morvan D, Dupuy JL, Porterie B, Larini M (2000) Multiphase formulation applied to the modelling of fire spread through a forest fuel bed. Proc Combust Instit 28:2803–2809
46. Mell W, Maranghides A, McDermott R, Manzello SL (2009) Numerical simulation and experiments of burning Douglas fir trees. Combust Flame 156:2023–2041
47. Katul GG, Mahrt L, Poggi D, Sanz Ch (2004) One and two equations models for canopy turbulence. Boundary Layer Meteorol 113:81–109
48. Tachajapong W, Lozano J, Mahalingam S, Zhou X, Weise D (2008) An investigation of crown fuel bulk density effects on the dynamics of crown fire initiation. Combust Sci Technol 180:593–615
49. Coelho PJ (2007) Numerical simulation of the interaction between turbulence and radiation in reactive flow. Prog Energy Combust Sci 33:311–383
50. Béguier C, Dekeyser I, Launder BE (1978) Ratio of scalar and velocity dissipation time scales in shear flow turbulence. Phys Fluid 21:307–310
51. Schiestel R (2006) Méthodes de modélisation et de simulation des écoulements turbulents. Lavoisier, Paris
52. Magnussen BF, Hjertager BH (1976) On mathematical modeling of turbulent combustion with special emphasis on soot formation and combustion. Proc Combust Instit 16:719–729
53. Magnussen BF, Hjertager BH, Olsen JG, Bhaduri D (1978) Effects of turbulent structure and local concentrations on soot formation and combustion in C2H2 diffusion flames. Proc Combust Instit 17:1383–1393
54. Clark MM, Fletcher TH, Linn RR (2010) A sub-grid, mixture-fraction-based thermodynamic equilibrium model for gas phase combustion in FIRETEC: development and results. Int J Wildland Fire 19:202–212
55. Mell W, Charney JJ, Jenkins MA, Cheney Ph, Gould J (2005) Numerical simulations of grassland fire behaviour from the LANL-FIRETEC and NIST-WFDS models. Proceeding of EastFIRE conference, George Mason University, Fairfax, VA, 11–13 May 2005

56. Dupuy JL, Marechal J, Morvan D (2003) Fires from a cylindrical forest fuel burner: combustion dynamics and flame properties. Combust Flame 135:65–76
57. Catchpole WR, Catchpole EA, Butler BW, Rothermel RC, Morris GA, Latham DJ (1998) Rate of spread of free-burning fires in woody fuels in a wind tunnel. Combust Sci Tech 131:1–37
58. Cheney NP, Gould JS, Catchpole WR (1993) The influence of fuel, weather and fire shape variables on fire-spread in grasslands. Int J Wildland Fire 3(1):31–44
59. Cheney NP, Gould JS (1995) Fire growth in grassland fuels. Int J Wildland Fire 5(4):237–247
60. Cheney NP, Gould JS, Catchpole WR (1998) Prediction of fire spread in grasslands. Int J Wildland Fire 8(1):1–13
61. Linn RR, Cunningham Ph (2005) Numerical simulations of grass fires using a coupled atmosphere-fire model: basic fire behaviour and dependence on wind speed. J Geophys Res 110:D1310719 pp
62. Mc Arthur (1976) Grassland fire danger meter MKV. CSIRO division of forest annual report 1976–1977, p 58
63. Sauer JA, Linn RR (2009) Higrad/Firetec, Multiple fuel types: approach, implementation and idealized scenarios. In: 8th Symposium on fire and forest meteorology, Kalispell, Montana USA, 13–15 October 2009
64. Mandel J, Bennethum LS, Beezley JD, Coen JL, Douglas CC, Kim M, Vodacek A (2008) A wildland fire model with data assimilation. Math Comput Simul 79:584–606
65. Filippi JB, Bosseur F, Mari C, Stradda S (2009) Numerical experiments using MESONH/FOREFIRE coupled atmospheric model. In: 8th Symposium on fire and forest meteorology, Kalispell, Montana USA, 13–15 October 2009
66. Andrews PL, Bevins CD (2003) In: Proceeding of the 2nd international congress on wildland fire ecology and fire management. 5th Symposium on fire and forest meteorology